Available online at www.sciencedirect.com
ScienceDirect
ELSEVIER
JOURNAL OF RARE EARTHS, Vol. 31, No. 2, Feb. 2013, P. 209
JOURNAL OF RARE EARTHS
www.re-journal.com/en/

Influence of $LaCl_3$ addition on microstructure and properties of nickel-electroplating coating

WANG Dan (王 丹), CHENG Yanfang (成艳芳), JIN Huiming (靳惠明)*, ZHANG Jiqun (张骥群), GAO Jicheng (高吉成)

(College of Mechanical Engineering, Yangzhou University, Yangzhou 225127, China)

Received 4 July 2012; revised 4 December 2012

Abstract: The influence of rare earth chloride $LaCl_3 \cdot 7H_2O$ addition on the microstructural features, phase structure, corrosion resistance and microhardness of nickel-electroplating was investigated. The Watts-type with different additive amounts of $LaCl_3 \cdot 7H_2O$ (0–1.2 g/L) were used in the experiment. Surface morphologies of coatings were examined by scanning electronic microscopy (SEM), transmission electronic microscopy (TEM) was used to measure the coatings' grain size and the microstructure of coatings was detected by X-ray diffraction (XRD). Corrosive investigation was carried out in 3.5 wt.% NaCl solution. The microhardness values of the coatings with different amounts of $LaCl_3 \cdot 7H_2O$ were measured, and the mechanism of the variation in microhardness was studied. Results showed that the addition of rare earth lanthanum refined the grain size and improved the surface consistency of the coatings, meanwhile the microhardness and corrosion property of coatings were improved and achieved a maximum with arround 1.0 g/L $LaCl_3 \cdot 7H_2O$ addition in electrolyte. The preferred growth orientation of lanthanum doped coating was crystal face (200), meanwhile the La_2Ni_7 phase was detected in the nickel coating by XRD and this was due to the induced co-deposition of elements La and Ni. The reason maybe was that the special out-layer electronic structure of element La raised the polarization of Ni cathode deposition, accelerated the nucleation of Ni and reduced hydrogen evolution from cathode surface.

Keywords: nickel-electroplating; lanthanum chloride; microstructure; corrosion; microhardness; rare earths

Electroplating nickel coating has been widely investigated and used due to its excellent corrosion resistance, wear resistance and high hardness. Its chemical and mechanical properties depend much on its microstructure. Most of the earlier studies on electroplating nickel coating have focused on addition of soluble salt, granular oxide and electroplating parameters. Meenu et al.[1] studied the changes in microstructure and corrosion behavior of eletrodeposited nickel with respect to cobalt addition. Atanassov et al.[2] found that the inclusion of manganese in the electrolyte led to the increase of internal stress and microhardness of the nickel layers and substantial decrease of plasticity. Zhao et al.[3] found that the incorporation of Cr particles enhances the microhardness and wear resistance of Ni coatings.

Rare earth (RE) elements, with many special physical and chemical properties, have been successfully used in many fields such as chrome coating, composite coating and other surface modification technology. Wang et al.[4] investigated the characteristics of Ni-W-B composites containing CeO_2 nano-particles prepared by pulse electrodeposition. Zhou et al.[5] studied the microstructure and depositional mechanism of Ni-P coatings with nano-ceria particles by pulse eletrodeposition. Wang et al. studied the amorphous rare-earth films of Ni-RE-P (RE=Ce, Nd) prepared by electrodeposition from an aqueous citric bath[6]. However, there is still little published work on the application of RE in nickel coating and their probable influence on depositing mechanism. In our earlier work, we have investigated that effects of lanthanum ion-implantation on microstructure of oxide film formed on Co-Cr alloy, structural characterization and corrosive property of Ni-P/CeO_2 composite coating and influence of nanometric ceria coating on oxidation behavior of chromium at 900 ºC[7–9]. In this study, rare earth lanthanum was added to Watts coating bath and the coatings' surface morphology, micro-grain size, surface microhardness, corrosion resistance, preferred growth orientation of nickel crystal and their correlation with lanthanum content added in electrochemical bath were studied.

1 Experimental

1.1 Material

A modified Watts-type Ni bath and the electroplating process conditions are presented in Table 1. The lanthanum chloride $LaCl_3 \cdot 7H_2O$ was used as additive and the contents used in the experiment was ranged from 0 to

Foundation item: Project supported by the Natural Science Foundation of Jiangsu Province (07KJD430246)

* **Corresponding author:** JIN Huiming (**E-mail:** doctorjhm@163.com; **Tel.:** +86-514-87978377)

DOI: 10.1016/S1002-0721(12)60260-9

Table 1 Bath formula and process parameters

Parameters	Dosage/value
$NiSO_4·6H_2O$/(g/L)	250
$NiCl_2·6H_2O$/(g/L)	50
H_3BO_3/(g/L)	35
$C_{12}H_{25}SO_4Na$/(g/L)	0.1
Saccharin/(g/L)	0.8
$LaCl_3·7H_2O$/(g/L)	0–1.2
pH	4.2
Pulse frequency/Hz	1000
Current density/(A/dm^2)	1.0
T/ºC	30±2
Duty cycle/%	50

1.2 g/L as enumerated in Table 1. All reagents used in the experiment were analytic grade. The pH of electrochemical bath was adjusted to appropriate value with $NH_3·H_2O$ (10 wt.%) and H_2SO_4 (10 wt.%) solutions.

Low carbon mild sheet (20 mm×15 mm×2 mm) specimens were used as the substrate, the working surfaces of which were finally ground by 1000# SiC abrasive paper and ultrasonically cleaned in alcohol and acetone, and the non-working surface insulated by insulating varnish. A high purity (99.99%) nickel plate was used as the soluble anode, the surface area of which was chosen approximately five times greater than that of the cathode to ensure that no problem would arise from the anodic polarization of nickel, particularly at high current densities. The equipments used in the electroplating progress are drawn in Fig. 1.

1.2 Characterization

Scanning electron microscopy (XL-30ESEM, PHILIPS) was used to examine the surface morphology while the grain size was studied by a transmission electron microscope (TECNAI 12 TEM, PHILIPS); The preferred growth orientation of coatings was detected by XRD (D8 ADVANCE, AXS) and Scherrer Equation was used to verify the grain size; Vickers microhardness tester (MVC-1000D1) was used to measure the microhardness; Tafel corrosion polarization curve of different coatings was measured in 3.5 wt.% NaCl solution by CP5 potentiostat.

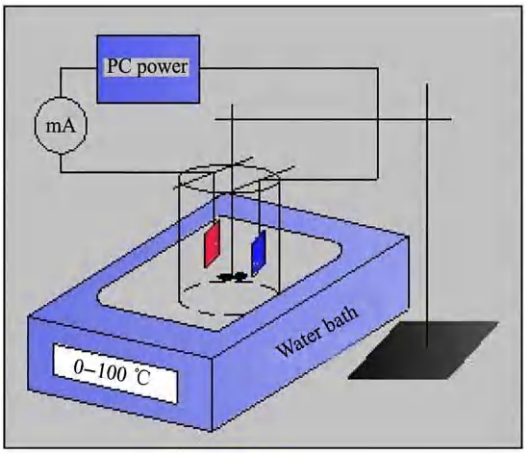

Fig. 1 Schematic diagram of experimental equipments (operating temperature range: 0–100 ºC)

2 Results and discussion

2.1 Surface morphology of coatings

Fig. 2(a) and (b) are the SEM images of pure nickel coating and lanthanum doped nickel coating ($LaCl_3·7H_2O$ content is 1.0 g/L in the bath), respectively. It can be seen that the SEM images of the nickel coating without lanthanum additive turns out to be colony-like morphology. It consists of a lot of grains colonies, and each colony consists of several smaller grain colonies, and the surface appears coarse and with many micropores on it, thus it can be corroded easily in corrosive environment. While the grains colonies of lanthanum-added are obviously refined and there are no obvious defects found on its outer surface, the coating's surface structure is more compact and significantly better than that of the pure nickel coating. Considering from the grain size, the quality of the coating containing rare earth elements was investigated by TEM images in Fig. 3(a) and (b). It can be seen from Fig. 3(a) that the grain size of pure nickel is about 60–80 nm while Fig. 3(b) shows that the grain size of the lanthanum doped coating is about 35–45 nm. We can see that the grain size is significantly refined after doping rare earth lanthanum. Besides, the electron diffraction pattern of lanthanum doped nickel coating indicates the presence of a polycrystal structure, and grain number of lantha-

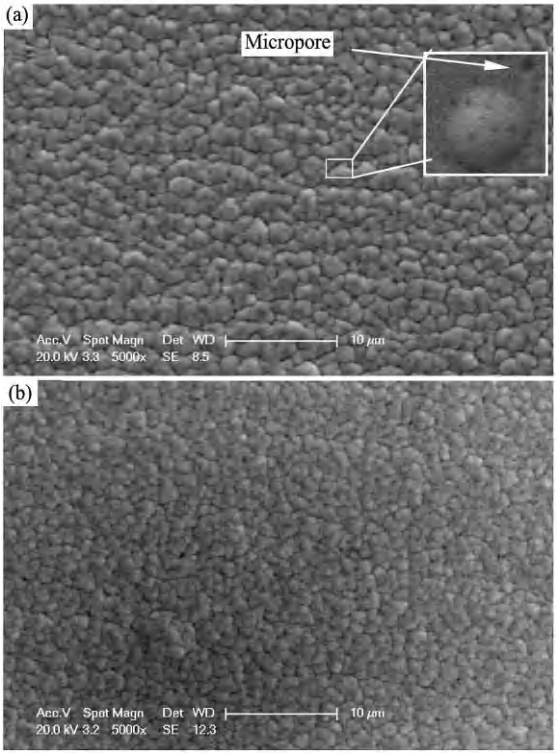

Fig. 2 SEM images of coatings
(a) Pure nickel coating; (b) Lanthanum doped nickel coating

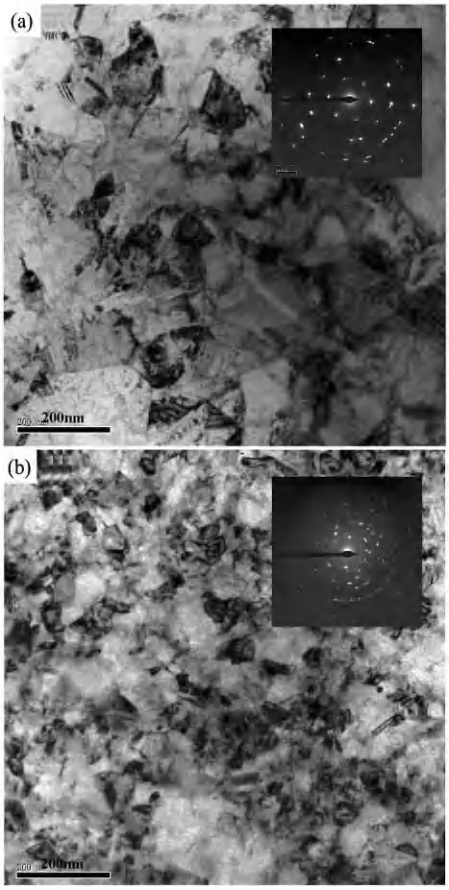

Fig. 3 TEM images of coatings
(a) Pure nickel coating; (b) Lanthanum doped nickel coating

num doped nickel coating is significantly more than pure nickel coating.

The refinement of grain size and the improvement of surface compaction not only enhances the mechanical properties of coatings, but also are beneficial to the coatings' corrosion resistance. These excellent properties of lanthanum doped nickel coating can mainly be attributed to the three effects of rare earth element on the electrochemical depositing process. Firstly, as we all know that the process of deposition is mainly that the cation is adsorbed on the surface of cathode. La is surface active element with a rather large atomic radius (radius of lanthanum is 0.1877 nm), and the outer layer electronic structure of lanthanum means that the La^{3+} is more easily adsorbed on the surface of cathode. When the plating process begins, Ni^{2+} is reduced on the surface of cathode, but La^{3+} almost does not participates the reaction, the loss of positive charge should be supplied by the new cations (La^{3+}, Ni^{2+}), so the content of Ni^{2+} in the electric double layer decreases as well as the increase content of La^{3+} , and it obstructs supply and reduction of Ni^{2+} in the bath, this process can be seen in Fig. 4 shown in the form of schematic diagram, so it needs a high overpotential to provide the energy of Ni^{2+} reduction thus alter the deposition of Ni^{2+} and refine the grain size[6]; Secondly, the overpotential also reduces the hydrogen evolution from

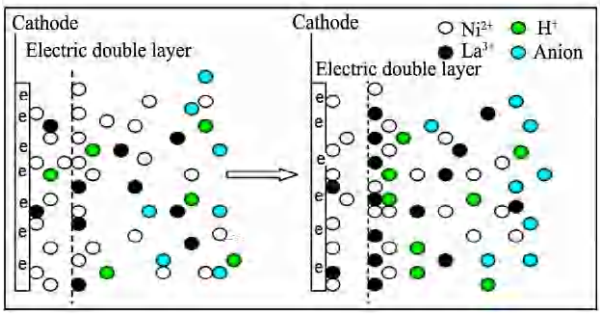

Fig. 4 Schematic diagram of the cathode reaction

the cathode surface, so that reduces the hydrogen embrittlement and pin holes and makes perfect surface integrity. Thirdly, the outermost electronic structure of rare earth lanthanum makes lanthanum ion adsorbed on the surface of cathode, that need to increase the cathodic potential to supply the Ni^{2+} reduction energy, thus increases the speed of new crystal nuclei's formation, and then refines grains[10].

Fig. 5 is EDS analysis of grain boundary of lanthanum doped nickel coating by Line Scanning (LS). The results show that the content of nickel is 99.73% and the content of La is little (It will be not precise when the content is below 0.5%). The reason of the results is that the experiment conditions dissatisfy the co-deposition of rare ear elements and other metallic elements: (1) existence of complexing agent to shift potential positively, (2) induction of transition ions. So the additive $LaCl_3 \cdot 7H_2O$ only alters the deposition mechanism of coating, and there is little or none into the coating.

2.2 Microstructure and phase of coatings

The influence of lanthanum addition on the preferred orientation of coating can be seen from the XRD (Cu Kα, λ=0.15406 nm) spectrum of pure nickel coating and lanthanum doped coating patterns as shown in Fig. 6. It can be seen that both coatings exhibit face-centered cubic (fcc) lattice but with different preferred orientations. Both coatings have apparent high diffraction peak generated from the Ni(111) and (200) crystal face, pure nickel coating has preferential growth of crystal face (200) trend slightly higher than that of (111) face, but the crystal face (200) of lanthanum doped coating is significantly enhanced, and the peak height of crystal face (200) is about 3 times of the peak height of (111) crystal face. Besides, the half width ratio of diffraction peaks of lanthanum doped coating is smaller than pure nickel. It is the evidence that lanthanum additive in electrolyte can refine the grain of coating. Meanwhile, it is also found that two little peaks are reduced because of the adding of lanthanum. This phenomenon may be attributed to the adsorption of lanthanum ion on the "growing point" of those crystal faces.

The coatings' grain size was also approximately calculated by the Scherrer's formula as in Eq. (1),

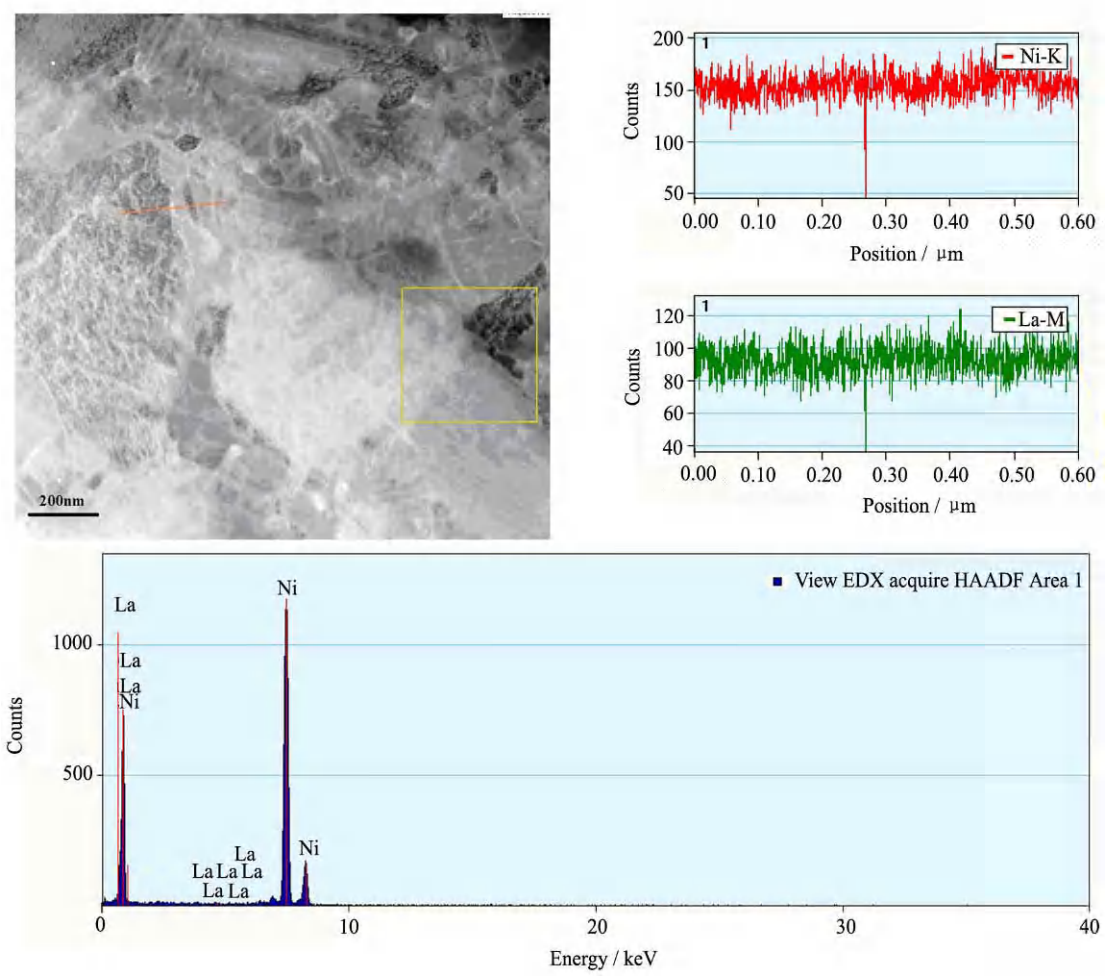

Fig. 5 EDS analysis of rare earth doped plating

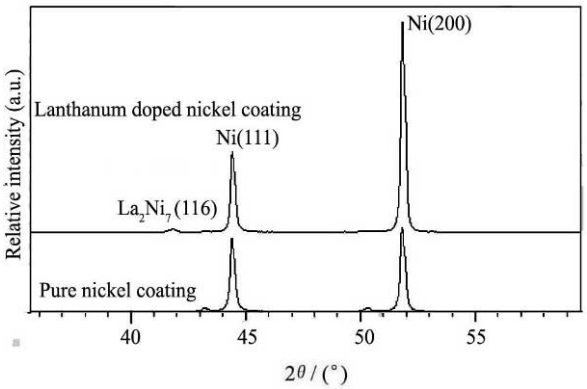

Fig. 6 XRD spectrum of coatings

$D_c=0.89\lambda/(B\cos\theta)$ (1)

Where λ is X-ray wavelength, B FWHM of diffraction peak, and θ the diffraction angle. The grain size of pure nickel coating is about 75 nm, while the grain size of lanthanum doped coating is about 40 nm, and these calculated grain size are approximately consistent with the grain size observed from the TEM images in Fig. 3. By analyzing the XRD spectrum, it is also found that some of the lanthanum ions enter into the coating and co-deposit with nickel ion forming the La_2Ni_7 phase, the content of which is about 0.13 wt.% in the coating. Because the lanthanum ion is difficult to be reduced to metal form, so only a little of its ions can co-deposit with nickel ions to form the lanthanum nickel inter-metallic compound.

2.3 Corrosion test

The Tafel polarization curves for Ni electroplating in the absence and presence of the rare earth element additive. There are five kinds of coatings in 3.5 wt.% NaCl solution which are shown in Fig. 7. Saturated calomel electrode (SCE) is used as the reference electrode and the potential dynamic scanning rate is 2 mV/s. It can be seen that the corrosion current of the nickel coating gradually decreases and the self-corrosion potential gradually shifts to the positive direction with increasing the content of $LaCl_3{\cdot}7H_20$ added in the bath. According to Table 2, when the additive content of $LaCl_3{\cdot}7H_20$ is 1.0 g/L in the bath, the coating's self-corrosion current decreases to the minimum value of 3.735×10^{-7} A/cm^2, and the self-corrosion potential reached a maximum value of –0.731 V, which represents the best anti-corrosion status of nickel coating. However, it should also be pointed out that when the additional quantity of $LaCl_3{\cdot}7H_20$ is too high, for example, when the content is 1.2 g/L, the corro-

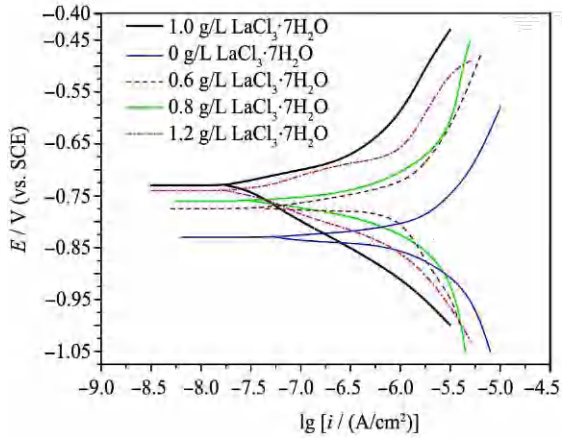

Fig. 7 Tafel polarization curves of five kinds of nickel coatings

Table 2 Self-corrosion conditions under different lanthanum contents

$LaCl_3·7H_2O$/(g/L)	Self-corrosion potential (V)	Self-corrosion current/(A/cm^2)
0	–0.831	1.584×10^{-6}
0.6	–0.776	1.122×10^{-6}
0.8	–0.753	7.070×10^{-7}
1.0	–0.731	3.735×10^{-7}
1.2	–0.742	5.620×10^{-7}

sion current of nickel coating turns larger and the corrosion potential shifts to the negative direction compared with 1.0 g/L $LaCl_3·7H_2O$ in the bath. Therefore, the lanthanum addition of appropriate content in the electrochemical bath can improve the corrosion resistance of Ni coating, and the optimum adding quantity of $LaCl_3·7H_2O$ is 1.0 g/L.

The corrosive property improvement can be attributed to surface integrity difference and structural difference. As our investigation on SEM images of pure coating and lanthanum doped coatings, the surface of RE coatings is more compact, less micropores and the grain of RE coating is finer than pure coating, the improvement of the quality of coating leads to the corrosive property improvement. So the corrosive property is increased with the increasing of RE content, and the corrosive property of RE coatings has a maximum with 1.0 g/L $LaCl_3$ addition in electrolyte.

2.4 Microhardness of coating

The microhardness of nickel coatings with different $LaCl_3·7H_2O$ doping contents was measured and are enumerated in Table 3. After doping lanthanum additive, the microhardness of lanthanum doped coating is visibly higher than that of the pure nickel coating. With the doping content of $LaCl_3·7H_2O$ increasing, the microhardness of coating is gradually enhanced. When the additive content reaches to 1.0 g/L, the maximum Vickers microhardness value is 397.67 kg/mm^2. When the $LaCl_3·7H_2O$ doping content is further to rise, it can be found that the coating's microhardness has a slight decrease. The doping of $LaCl_3·7H_2O$ helps to enhance the microhardness of the coating but the content of $LaCl_3·7H_2O$ must be strictly controlled. And 1.0 g/L is the optimum content.

Table 3 Microhardness under different lanthanum contents

$LaCl_3·7H_2O$/(g/L)	0	0.6	0.8	1.0	1.2
Microhardness/(kg/mm^2)	217.23	321.51	357.20	397.67	384.53

According to Hall-Petch law (HPL), the microhardness of coatings will increase with the refinement of grain size. The relationship between the yield stress (or microhardness) and the grain size, based on the dislocation pile-up theory of nanocrystalline or polycrystalline materials, can be expressed as

$$\sigma=\sigma_0+K_H\cdot d^n \quad (2)$$

Where σ is macro yield stress, σ_0 is lattice friction to be overcome when removing a single dislocation, K_H is constant, d is the average grain diameter, and n is the exponent of grain size, usually is −1/2. But, this relationship has some limitations: Firstly, strength will not grow unlimitedly to exceed the theoretical restrictions; Secondly, any relaxation processes on crystal boundary may result in the reduction of microhardn ess, so the phenomenon of inverse HPL will appear in a critical grain size; Thirdly, HPL is theoretically based on dislocation pile-up theory, when the grains are ultrafine, the individual grain could not produce multiple dislocation pile-up, the HPL will be invalid[11]. In our experiment, when $LaCl_3·7H_2O$ content in the bath is less than 1.0 g/L, the grain size of coating is relatively large and satisfies the HPL theory, and the microhardness will increase; And when $LaCl_3·7H_2O$ content in the bath is more than 1.0 g/L, the microhardness of the deposits decreases which can be correlated to the "inverse HPL effect"[12].

3 Conclusions

Additions of rare earth chloride $LaCl_3·7H_2O$ to electroplating nickel coating resulted in the followings conclusions:

(1) Nickel coatings prepared by adding lanthanum chloride in the electrolyte turned out to be better surface quality with more compact, less micropores.

(2) The optimum addition of $LaCl_3·7H_20$ in this study was 1.0 g/L and the microstructure was refined.

(3) According to X-ray diffraction, it could be found that both coating had apparent high diffraction peak generated from the Ni(111) and (200) crystal face, pure nickel coating had preferential growth of crystal face (200), and the preferred growth orientation of lanthanum doped coating's crystal face (200) was significantly enhanced. Meanwhile, a very small amount of lanthanum ions co-deposited with nickel ions in the coating as the La_2Ni_7 phase.

(4) The corrosion resistance and microhardness of coating with 1.0 g/L $LaCl_3·7H_20$ in the bath was the highest.

References:

[1] Meenu S, Ezhil Selvi V, William Grips V K, Rajam K S. Corrosion resistance and microstructure of electrodeposited nickel-cobalt alloy coatings. *Surf. Coat. Technol*., 2006, **201**: 3015.

[2] Atanassov N, Mitreva V. Electrodeposition and properties of nickel-manganese layers. *Surf. Coat. Technol*., 1996, **78**: 144.

[3] Zhao G G, Zhou Y B, Zhang H J. Sliding wear behaviors of electrodeposited Ni composite coatings containing micrometer and nanometer Cr particles. *Trans. Nonferrous Met. Soc. China*, 2009, **19**: 319.

[4] Wang J L, Xu R D, Zhang Y Z. Study on characteristics of Ni-W-B composites containing CeO_2 nano-particles prepared by pulse electrodeposition. *J. Rare Earths*, 2012, **30**(1): 43.

[5] Zhou X W, Shen Y F, Jin H M, Zheng Y Y. Microstructure and depositional mechanism of Ni-P coatings with nano-ceria particles by pulse electrodeposition. *Trans. Nonferrous Met. Soc. China*, 2012, **22**: 1981.

[6] Wang L L, Tang L M, Huang G F, Huang W Q, Peng J. Preparation of amorphous rare-earth films of Ni-Re-P (Re=Ce, Nd) by electrodeposition from an aqueous bath. *Surf. Coat. Technol*., 2005, **192**: 208.

[7] Jin H M, Zhou X W, Zhang L N. Effects of lanthanum ion-implantation on microstructure of oxide film formed on Co-Cr alloy. *J. Rare Earths*, 2008, **26**(3): 406.

[8] Jin H M, Jiang S H, Zhang L N. Structural characterization and corrosive property of Ni-P/CeO2 composite coating. *J. Rare Earths*, 2009, **27**(1): 109.

[9] Jin H M, Liu X J, Zhang L N. Influence of nanometric ceria coating on oxidation behavior of chromium at 900 °C. *J. Rare Earths*, 2007, **25**(1): 63.

[10] Wang D L, Wang C Y, Dai C S. Study of Co-Ce coating and surface on pasted nickel electrodes substrate. *Rare Met*., 2006, **25**(10): 47.

[11] Liu Y, Luo Y H, Wei Z D. Current status of pulse plating research. *Plat. Surf. Finish*., 2005, **27**(5): 25.

[12] Chen Y R, Long J M, Pei H Z. Research status Quo and future prospects of nickel and nickel alloys pulse electro-deposition. *Plat. Surf. Finish*., 2009, **31**(2): 16.